Article citation info:
OPALIŃSKI, M., TEODORCZYK, A., KALKE, J. The closed-cycle model numerical analysis of the impact of crank mechanism design on engine efficiency. *Combustion Engines*. 2017, **168**(1), 153-160. DOI: 10.19206/CE-2017-125

Marcin OPALIŃSKI
Andrzej TEODORCZYK
Jakub KALKE

CE-2017-125

The closed-cycle model numerical analysis of the impact of crank mechanism design on engine efficiency

The research presents a review and comparison of different engine constructions. Investigated engines included crankshaft engines, barrel engine, opposed-piston engines and theoretical models to present possible variations of piston motion curves.

The work comprises also detailed description of a numerical piston engine model which was created to determine the impact of the cycle parameters including described different piston motion curves on the engine efficiency. Developed model was equipped with Wiebe function to reflect a heat release during combustion event and Woschini's correlation to simulate heat transfer between the gas and engine components.Various scenarios of selected engine constructions and different working conditions have been simulated and compared. Based on the results it was possible to determine the impact of different piston motion curves on the engine cycle process and present potential efficiency benefits.

Key words: *piston motion, engine, simulation, efficiency, opposed*

1. Introduction

Most of the recent piston engines which are used in all types of business (automotive, aviation, marine and power) are presenting typical crankshaft mechanism where piston is connected to the crank shaft through a piston rod. Some of the constructions (e.g. RND 105 marine engine) includes additional connecting rod between the piston rod and crank shaft in order to decrease the piston side force but this design does not differ significantly from the first one in regards to the piston motion curve. Apart from that construction more and more companies are interested in new piston engine constructions. Most remarkable designs are those which are based on the opposed-piston (OP) engine concept. This design in general may provide reduced fuel consumption or increased power-to-weight ratio.

There are six main types of the OP engines [1]:

1. Crankless free piston engine
2. Single Crankshaft engines
3. Double Crankshaft engines
4. Multi Crankshaft engines
5. Rotary engines
6. Barrel engines

All of those constructions may be additionally divided for subtypes since there are different variants of the joints which can be applied for those engines.

This work focuses on the impact of different constructions on the piston motion. Different piston motion have impact on the local piston speed and thus the heat transfer. Also the different piston motion result in the different pressure profile, pressure derivative and therefore efficiency and other factors. Eight different construction have been selected to analyze the effect of different crank mechanism designs on the engine efficiency.

2. Review of different engine constructions

Selected engine construction for the analysis includes: typical crank shaft mechanism (STDE), crank shaft mechanism with added cam rod (EE), barrel engine (BE), single shaft opposed-piston engine (SSOP), single shaft OP engine with phasing (SSPOP), double shaft OP engine (DSOP), opposed piston barrel engine (BEOP) and the elliptical shape rotating cylinder (ERCOP). For each construction a piston motion equation was presented in subchapters 2.1–2.8.

2.1. Traditional crank shaft mechanism (STDE)

This design is world wide spread in all types of industries as it was stated at the beginning of the work. This construction will be used as the baseline for comparison purposes.

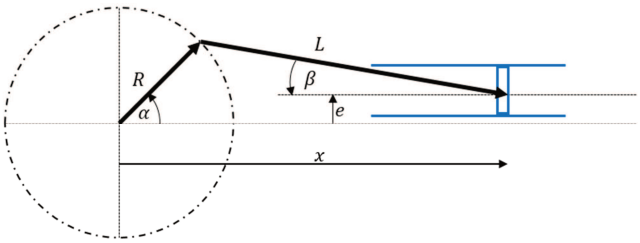

Fig. 1. STDE engine scheme

The equation for piston movement is as follows [2, 3]:

$$x = R\left(\cos\alpha + \frac{1}{\lambda}\sqrt{1-(\lambda\sin\alpha-\mu)^2}\right) \quad (1)$$

where: x – piston location, R – distance between crankshaft axis and piston rod crankshaft joint, L – length of the piston rod, α – crankshaft angle (CA), λ – is the R/L ratio, μ – is the e/L ratio.

The piston stroke may be directly calculated using following equation:

$$s = R\left(\sqrt{\left(\frac{1}{\lambda}+1\right)^2-\left(\frac{\mu}{\lambda}\right)^2}-\sqrt{\left(\frac{1}{\lambda}-1\right)^2-\left(\frac{\mu}{\lambda}\right)^2}\right) \quad (2)$$

2.2. Crank shaft mechanism with cam rod (EE)

This model of the engine was proposed by Rychter and Teodorczyk in 1985. The main advantage of this construction was variable compression ratio. The idea of this engine was to introduce additional eccentric rod between the crankshaft and piston rod with possible rotational move-

ment during engine work. The concept was analyzed for different relative rotational speeds between the crankshaft and eccentric rod [3–5].

1. $\omega_{rod} = \omega_{crankshaft}$
2. $\omega_{rod} = \pm\frac{1}{2}\omega_{crankshaft}$
3. $\omega_{rod} = \pm\omega_{crankshaft}$

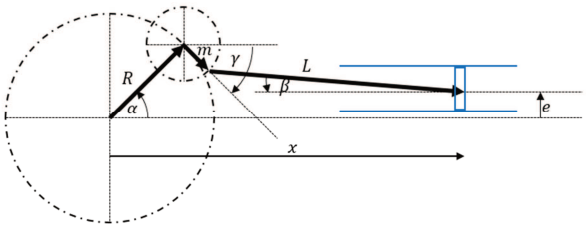

Fig. 2. EE engine scheme

For this engine the the piston motion curves is represented by following equation:

$$x = R\left(\cos\alpha + \frac{\delta}{\lambda}\cos\gamma + \frac{1}{\lambda}\sqrt{1-(\lambda\sin\alpha - \delta\sin\gamma - \mu)^2}\right) \quad (3)$$

where: m – length of the eccentric rod, δ – is the m/L ratio, other parameters are the same as for the STDE.

2.3. Barrel engine (BE)

The barrel engine, known also as axial engine, is a construction where cylinders are parallel to the crankshaft. This construction may be realized by cam, swash plate or wobble plate.

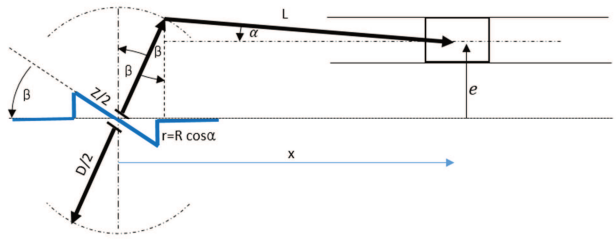

Fig. 3. BE engine scheme

Derived equation for the piston movement is expressed by the following formula:

$$x = \frac{DR\cos\alpha}{Z} + L\sqrt{1-\left(\frac{\frac{D}{2}\sqrt{1-\left(\frac{2R\cos\alpha}{Z}\right)^2}-e}{L}\right)^2} \quad (4)$$

where: Z – length of the crank, D – plate diameter, R – crank radius, e – distance between shaft axis and cylinder axis.

The stroke of the engine is represented by the formula:

$$s = 2\frac{DR}{Z} \quad (5)$$

2.4. Single shaft opposed-piston engine (SSOP)

The construction of SSOP engine reaches XIX century [1]. Single crankshaft is connected to two pistons through two crank rods with different lengths. The longer rod provides pulling force after combustion while the shorter rod pushes in the same time. This ensures well balanced design. Recently that type of engine construction is developed by the Ecomotors company [6].

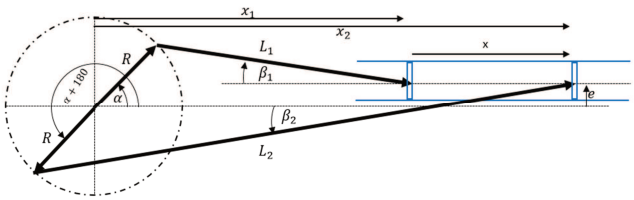

Fig. 4. SSOP engine scheme

The closed gas length is described by the following formula:

$$x = s - R\left(\frac{1}{\lambda_2}\sqrt{1-\lambda_2^2(\sin\alpha+\epsilon)^2} - 2\cos\alpha - \frac{1}{\lambda_1}\sqrt{1-\lambda_1^2(\sin\alpha-\epsilon)^2}\right) \quad (6)$$

where: λ_1, λ_2 – are ratios of $\frac{R}{L_1}$ and $\frac{R}{L_2}$ respectively, ϵ – is a ratio of $\frac{e}{R}$, other parameters are the same as for the STDE.

2.5. Single shaft opposed-piston engine with phasing (SSPOP)

This engine model is a derivative of the previous one. The concept provides additional geometrical parameters like different radii of the crankshaft (R_1, R_2) and angle shift between the cranks Δ.

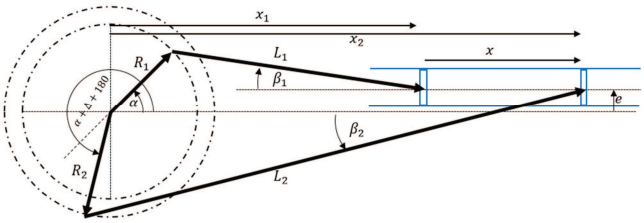

Fig. 5. SSPOP engine scheme

The equation for the captured gas length is:

$$x = s - R_2\left(\frac{1}{\lambda_2}\sqrt{1-\lambda_2^2(\sin(\alpha+\Delta)+\epsilon_2)^2} - \cos(\alpha+\Delta)\right) - R_1\left(\cos\alpha + \frac{1}{\lambda_1}\sqrt{1-\lambda_1^2(\sin\alpha-\epsilon_1)^2}\right) \quad (7)$$

where: λ_1, λ_2 – are the ratios $\frac{R_1}{L_1}$, $\frac{R_2}{L_2}$ respectively, ϵ_1, ϵ_2 – are the ratios $\frac{e}{R_1}, \frac{e}{R_2}$ respectively.

2.6. Double shaft opposed-piston engine (DSOP)

This type of engine contains two crankshafts which are driving via the piston rods two opposed pistons. Those shafts are coupled with gears, lay-shafts or chain to maintain the same movement. It is possible to provide in this construction phase shift for both crankshafts.

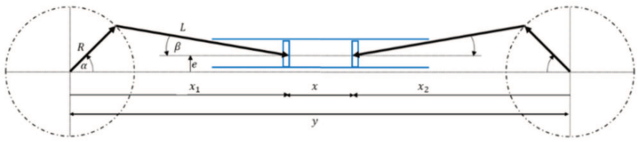

Fig. 6. DSOP engine scheme

The piston motion for this construction is the same as the motion for STDE engine with the difference that there are two pistons. So the geometrical parameters of the crankshaft construction are different for the same piston stroke. Additionally this construction may have for the same compression ratio and volume as the STDE lower piston speed for the same engine speed. Each of the piston from DSOP has to cover half of the distance with comparable STDE. That engine configuration is recently developed by the Achates Power company [7].

2.7. Opposed-piston barrel engine (BEOP)

This engine is a single shaft construction with all cylinders placed parallel to and around main shaft. The plates are located on opposite sides of the crankshaft.

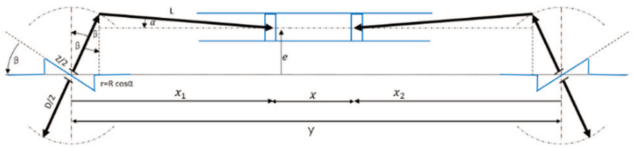

Fig. 7. BEOP engine scheme

The piston motion is the same as the BE construction with the same difference between the STD and DSOP - two pistons for one cylinder. This engine is recently developed at Warsaw University of Technology [8].

2.8. Elliptical rotating cylinder engine (ERCOP)

This engine is known also as a Coomber rotary engine [9] which was designed at the end of 19th century. The biggest advantage of this construction is elimination of piston side force and transferring it to the rollers which are moving on the elliptical guideway. The shape in general for that type of engine does not have to be an ellipse but this research will focus on that construction.

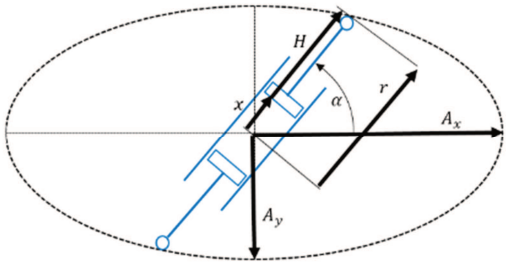

Fig. 8. ERCOP engine scheme

Derived equation for the combustion chamber lengths is presented by the formula:

$$x = \sqrt{\frac{A_y^2}{1-e^2\cos^2\alpha}} - H \tag{8}$$

where: A_y – the smallest ellipse radius, A_x – the biggest ellipse radius, H – the height of the piston with rollers, e – ellipse eccentricity described as:

$$e^2 = \frac{A_x^2 - A_y^2}{A_x^2} \tag{9}$$

Stroke can by calculated as the double difference between the maximum and minimum ellipse radii:

$$s = 2(A_x - A_y) \tag{10}$$

3. Piston motion curves

In order to compare all types of engines it was decided to provide for all constructions exactly the same geometrical dimensions. All models have the same piston bore, total piston stroke and compression ratio. Total piston stroke for all engines is the change of length of cylindrical volume of the gas for the compression and expansion process (maximum gas length decreased by minimum gas length). There was no differentiation between the compression and expansion ratios (like in the Atkinson cycle). It has to be noticed that for the opposed piston configuration determination of top dead center (TDC) and bottom dead center (BDC) may be addressed to the:

- minimal and maximal gas volume,
- TDC and BDC of the inlet piston position,
- TDC and BDC of the exhaust piston position,

For the need of this work the TDC and BDC will be associated with the gas volume regardless of the construction. The Table 1 presents selected engines' geometry parameters.

Table 1. Geometrical engine parameters for all configurations

Parameter	Unit	Value
Bore	mm	50
Stroke	mm	194
Volume of cyl	L	0.381

To obtain exactly the same stroke and CR for all engines the geometrical parameters were calculated based on the equations (1)–(10) prestented in the chapter 2. For those designs which stroke equation was not directly provided in this work the geometrical parameters were numerically determined to achieve required stroke and compression ratio. The stroke and compression ratio which were numericaly determined where accurate within 10^{-4}mm for stroke and 10^{-3} for CR.

The selected geometrical parameters were presetented in the Tables 2–9. All the parameters presented in the tables were rounded to 3 decimal places.

Table 2. Geometrical engine parameters for STDE

type	μ	λ	R
STDE_1	–0.1	0.2	96.493
STDE_2	–0.1	0.3	96.465
STDE_3	–0.1	0.4	96.420
STDE_4	0	0.2	97
STDE_5	0	0.3	97
STDE_6	0	0.4	97
STDE_7	0.1	0.2	96.493
STDE_8	0.1	0.3	96.465
STDE_9	0.1	0.4	96.420

The EE engine configuration presents very unique behaviour near the TDC. The compressed gas starts to expand for a while and just after TDC compresses once again. This situation appears when the angular position of the eccentric rod is twice bigger then crank angle ($\alpha_r = 2\alpha_c$). That means also that the eccentric rod rotates twice faster then crank angle.

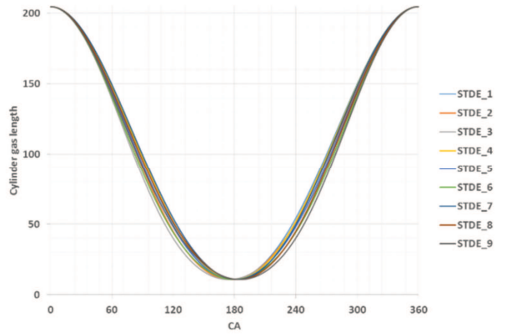

Fig. 8. STDE piston motion curves

Table 3. Geometrical engine parameters for EE

type	μ	λ	R	e_rod pos	δ
EE_1	–0.1	0.4	43.328	$\alpha_r = \alpha_c$	0.495
EE_2	–0.1	0.6	64.996	$\alpha_r = \alpha_c$	0.295
EE_3	–0.1	0.8	86.875	$\alpha_r = \alpha_c$	0.089
EE_4	0	0.4	42.135	$\alpha_r = 2\alpha_c$	0.544
EE_5	0	0.6	63.175	$\alpha_r = 2\alpha_c$	0.345
EE_6	0	0.8	84.272	$\alpha_r = 2\alpha_c$	0.144
EE_7	0.2	0.4	47.200	$\alpha_r = \alpha_c + 30^o$	0.567
EE_8	0.2	0.6	70.172	$\alpha_r = \alpha_c + 30^o$	0.365
EE_9	0.2	0.8	88.241	$\alpha_r = \alpha_c + 30^o$	0.136

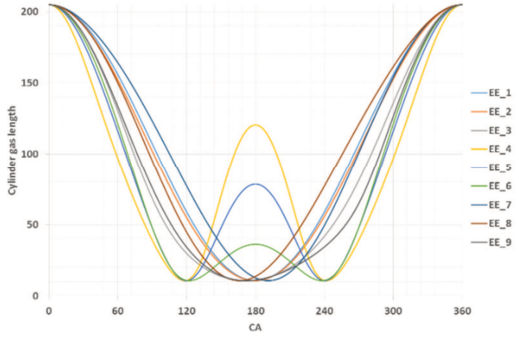

Fig. 9. EE piston motion curves

Table 4. Geometrical engine parameters for SSOP

type	λ_1	λ_2	R	ϵ
SSOP_1	0.2	0.148	48.493	–0.1
SSOP_2	0.3	0.196	48.485	–0.1
SSOP_3	0.4	0.234	48.493	–0.1
SSOP_4	0.2	0.148	48.485	0
SSOP_5	0.3	0.196	48.475	0
SSOP_6	0.4	0.234	48.5	0
SSOP_7	0.2	0.148	48.5	0.3
SSOP_8	0.3	0.196	48.5	0.3
SSOP_9	0.4	0.234	48.434	0.3

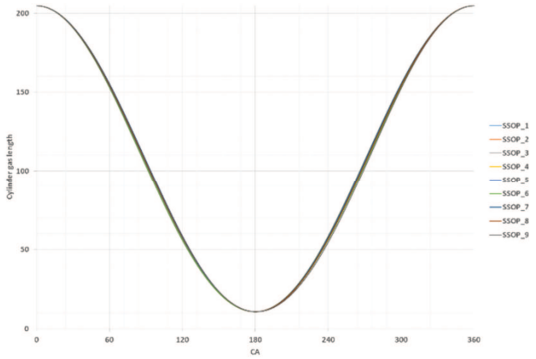

Fig. 10. SSOP piston motion curves

Table 5. Geometrical engine parameters for SSPOP

type	λ_1	λ_2	R_1	R_2	δ	ϵ_1	ϵ_2
SSPOP_1	0.225	0.193	45	55.312	–0.524	–0.1	–0.081
SSPOP_2	0.225	0.182	45	51.983	0	–0.1	–0.087
SSPOP_3	0.225	0.193	45	55.135	0.524	–0.1	–0.082
SSPOP_4	0.225	0.193	45	55.241	–0.524	0	0
SSPOP_5	0.225	0.182	45	52	0	0	0
SSPOP_6	0.225	0.193	45	55.241	0.524	0	0
SSPOP_7	0.225	0.193	45	55.135	–0.524	0.1	0.082
SSPOP_8	0.225	0.182	45	51.983	0	0.1	0.087
SSPOP_9	0.225	0.193	45	55.312	0.524	0.1	0.081

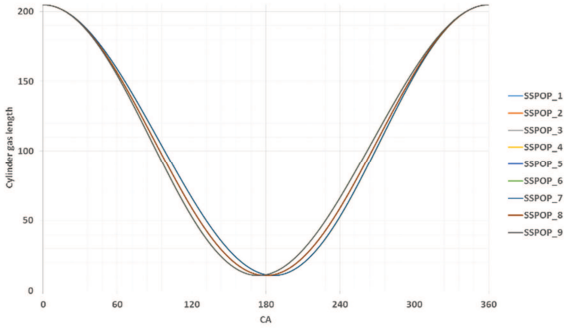

Fig. 11. SSPOP piston motion curves

Table 6. Geometrical engine parameters for ERCOP

type	A_x	A_y	H	e^2
ERCOP_1	400	303	297.611	0.426
ERCOP_2	350	253	247.611	0.477
ERCOP_3	300	203	197.611	0.542
ERCOP_4	250	153	147.611	0.625
ERCOP_5	200	103	97.611	0.735
ERCOP_6	150	53	47.611	0.875

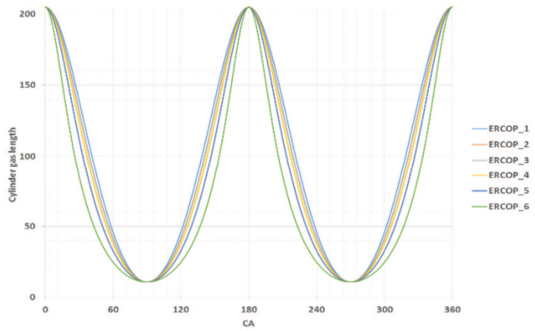

Fig. 12. ERCOP piston motion curves

Table 7. Geometrical engine parameters for BE

type	*Z*	*e*	*R*	*D*	*L*
BE_1	100	50	26.608	364.558	150
BE_2	100	75	23.789	407.759	150
BE_3	100	100	21.443	452.364	150
BE_4	200	100	42.886	452.364	150
BE_5	200	150	35.636	544.393	150
BE_6	200	200	30.368	638.822	150
BE_7	300	150	53.454	544.393	150
BE_8	300	225	42.381	686.629	150
BE_9	300	300	34.993	831.598	150

It can be noticed that during one rotation of the crankshaft there are 2 cycles of the engine for the ERCOP configuration. Due to significant difference between this piston motion and the rest of the engines it was decided to carry calculations such as only one compression and one

expansion appears in the piston motion for whole engine rotation. This can be comapared to the situation as if the ERCOP engine was working with twice lower engine speed then the other engines so the number of cycles within a particular time remains the same.

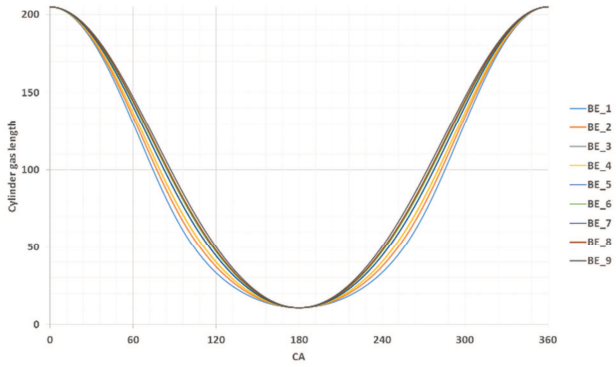

Fig. 13. BE piston motion curves

Table 8. Geometrical engine parameters for DSOP

type	μ	λ	R_1	R_2	ψ
DSOP_1	0.03	0.2	48.626	48.700	–10
DSOP_2	0.03	0.3	48.606	48.718	–10
DSOP_3	0.03	0.4	48.585	48.734	–10
DSOP_4	0.03	0.2	48.477	48.477	0
DSOP_5	0.03	0.3	48.476	48.476	0
DSOP_6	0.03	0.4	48.474	48.474	0
DSOP_7	0.03	0.2	48.626	48.700	10
DSOP_8	0.03	0.3	48.606	48.718	10
DSOP_9	0.03	0.4	48.585	48.734	10

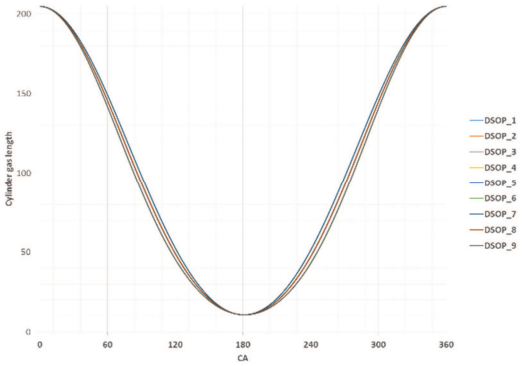

Fig. 14. DSOP piston motion curves

Table 9. Geometrical engine parameters for BEOP

type	Z	e	R	D	L
BEOP_1	100	50	12.367	392.157	150
BEOP_2	100	75	11.003	440.777	150
BEOP_3	100	100	9.905	489.675	150
BEOP_4	200	100	19.809	489.675	150
BEOP_5	200	150	16.496	588.027	150
BEOP_6	200	200	14.122	686.855	150
BEOP_7	300	150	24.744	588.027	150
BEOP_8	300	225	19.759	736.388	150
BEOP_9	300	300	16.435	885.301	150

Each of the engine piston motion curves for different geometrical parameters was presented in the Figures 8–15. Every equation for each engine was shifted in phase to maintain max gas volume at 0 deg CA. In most cases it resulted with the TDC apearing at 180 deg CA.

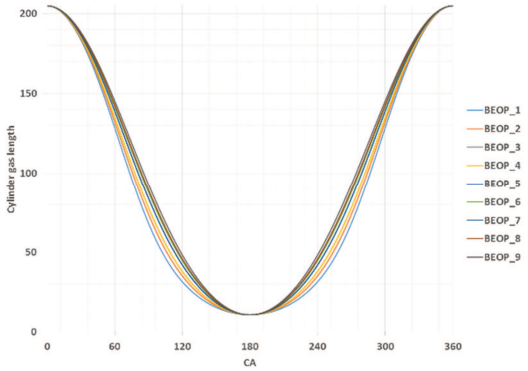

Fig. 15. BEOP piston motion curves

4. Model of the engine

All engines have been represented by a closed-cycle numerical model. The incylinder paramters where based on the ideal gas properties. The gas model was built based on the ideal gas mixture of the following species: nitrogen (N), oxygen (O_2), argon (Ar), carbon dioxide (CO_2), water (H_2O) and isooctane (C_8H_{18}). The molecular mass, volume and mass fractions where determined for each time step. The specific heat of the gas was determined based on the polynomal equations provided by NASA spec [10]. Pressure prediction was modeled by the following formula

$$\frac{dp_i}{d\Theta_i} = \left(\frac{dQ_{c,i}}{d\Theta_i} - \frac{dQ_{ht,i}}{d\Theta_i} - \frac{\gamma_i}{\gamma_i - 1} p_i \frac{dV_i}{d\Theta_i}\right) \frac{\gamma_i - 1}{V_i} \tag{12}$$

where: $\frac{dp_i}{d\Theta_i}$ – change of pressure at current step, $\frac{dQ_{c,i}}{d\Theta_i}$ – heat release at current step, $\frac{dQ_{ht,i}}{d\Theta_i}$ – heat transfer to walls at current step, $\frac{dV_i}{d\Theta_i}$ – change of gas volume at current step, p_i – current gas pressure, V_i – current gas volume, γ_i – current gas ratio of specific heats.

The model of the engine heat release was created based on the Woschni correlation with heat transfer coefficient described by the following formula:

$$h_{c,i} = 5 b^{m_{ht}-1} p_i^{m_{ht}} w_i^{m_{ht}} T_i^{0.75-1.62 m_{ht}} \tag{11}$$

where: b – pistone bore, p_i – pressure in current step, w_i – cylinder gas velocity in current step, T_i – gas temperature in current step, m_{ht} – constant equal to 0.8.

The combustion of the fuel mixture was based on complete combustion of isooctane with heat release based on the Wiebe expotential function:

$$x_{end,i} = 1 - \exp\left\{-\left[\left(2.302^{\frac{1}{m_c+1}} - 0.105^{\frac{1}{m_c+1}}\right)\left(\frac{\Theta_i - \Theta_{cstart}}{\Theta_{cdur}}\right)\right]^{m_c+1}\right\} \tag{12}$$

where: $x_{end,i}$ – amount of the fuel burned in particular time step, m_c – constant equal to 0.7, Θ_i – current angle (time), Θ_{cstart} – angle when 10% of fuel burned, Θ_{cdur} – duration of combustion from 10-90% of burned fuel.

The complete combustion model was based on the chemical reaction:

$$C_8H_{18} + 12.5O_2 \rightarrow 8CO_2 + 9H_2O \tag{13}$$

Fuel vapors were injected into the cylinder at the beginning of the engine cycle. The species' fractions and gas specyfic heat was updated for each additional fuel mass injected and timestep. The amount of fuel injected into the cylinder cycle starting paramters (p_0, T_0) and air-fuel equivalence ratio (λ). Based on that approach the amount of fuel injected for each engine is exactly the same when starting parameters are the same. Thus the power and efficiency of the engines depends mostly on the piston motion curve and combustion parameters. The power and efficiency were calculated based on the presented integral:

$$\eta_t = \frac{\int_{start}^{end} p_i dv_i}{m_{fuel} LHV} \tag{14}$$

where: p_i – is current gas pressure, dv_i – change of volume in calculation time step.

While the power of the engine was calculated based on the formula (2-stroke engine):

$$P = \eta_t m_{fuel}\, LHV\, N/60 \tag{15}$$

where: m_{fuel} – mass of fuel injected in one cycle, LHV-lower heat value of the fuel, N – engine speed.

There were 8 different configurations of engines investigated. Most of them were presented by 9 geometrical variations. In total there were 69 different piston motion curves implemented into the closed-cycle model. Two additional parameters have been selected to run calculations connected with the shape of the pressure profile in the cylinder: combustion duration (T_{cdur}) and start of combustion (T_{cstart}). The rest parameters remained unchanged. The Table 10 presents constant parameters for all engines calculations, while Table 11 presents 5 different setups for each piston motion curve, so in total there were 345 engine cases analyzed.

Table 10. Constant parameters for engine cycle simulations

Parameter	value	unit
Fuel lower calorific value (LHV)	47	MJ/kg
Air-fuel equivalence ratio (λ)	1.1	–
Engine speed	1500	rpm
Starting pressure	4	bar
Starting temperature	350	K
Mean piston surface temperature	580	K
Mean liner surface temperature	480	K
Volume content of water in air	1	%

Table 11. Variable parameters for engine cycle simulations

Setup	T_{cdur} (deg)	T_{cstart} (deg)
1	50	170
2	50	180
3	50	190
4	30	180
5	70	180

The closed cycle model did not include the scavenging process of the cylinder. The closed portion of volume of gas for each engine was exactly the same. The gas was 100% of fresh air (no residual gases) at the beginning and 100% of burned gas after combustion process.

5. Results

For each of the engine configuration and setup it was possible to plot the pressure, temperature, volume and all derivatives of the parameters for all timesteps. The major attention was paid to the engines' efficiency and power which were calculated with the equations 14 and 15.

From all results obtained for all engine configurations 3 of them were excluded. Those which excluded regarded 3 engine variations of configuration EE (particularly EE_4, EE_5 and EE_6). The calculations of these engine resulted in extremely high peak pressures (~700 bar) and peak temperatures (> 3000 K). For that high temperatures the amount of heat was so high that the heat losses exceeded fuel heat delivered. This unique engine design requires separate discussion to explain the reason of so high gas parameters.

Figure 16 presents a comparison of different engine configurations in regards to the efficiency. The presented efficiencies are the avarage efficiency of all engine geometrical variations for the particular combustion parameters setup (T_{cdur},T_{cstart}). For instance first column in Figure 16 presents the average efficiency of all gemetrical variations of STDE engine (STD_1, STD_2, …, STD_9) for the Setup 1 described in Table 11 (so for the T_{cdur} = 50 deg and T_{cstart} = 170 deg).

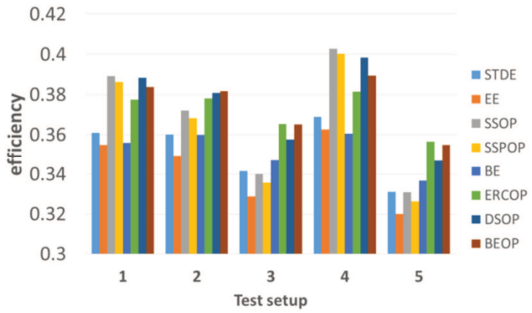

Fig. 16. Comparison of different setups on engine efficiencies

It can be noticed that the lowest engine efficiency was presented for the setup 5 by the EE engine (32.0%). The second lowest efficiency was also noticed for the setup 5 for the SSPOP engine configuration (32.6%). The highest efficiencies were observe for the SSOP engine and the second for the SSPOP, both for the latest combustion start (efficiency were equal to 40.3% and 40,0% respectively). It can be noticed that the behavior of the models was not linear. Higher impact on the efficiency was observed for the combustion duration (±20 deg variations) parameter than for the start of the combustion parameter (±10 deg variations). The BE engines presented lowest variations of efficiency which range was 33.7–36.0% for different setups.

The highest efficiency for the single engine configuration and variation was noted for the SSPOP_1. This model reached 40.6% for the setup 4. The lowest efficiency (excluding EE_5 to EE_7) for the particular variation was noted for the EE_8 configuration, setup 5 27.2%.

Figure 17 presents the comparison of averaged efficiency for all setups and variations for each design. Three lowest averaged efficiency are represented by the not opposed-piston configurations (STDE, EE, BE). This is connected with the reduced area of heat transfer for a cylinder (lack of engine head for OP designs). The difference between the BE and BEOP reaches 2.3 percentage points what gives 6.5% difference in regards to BE efficiency. Very similar

relative difference is between STDE and DSOP configurations. For those configuration the difference reaches 6.2%. The highest average efficiency was noted for the BEOP configuration (37.5%) with small difference to the DSOP engines (37.4%) and ERCOP engines (37.2%).

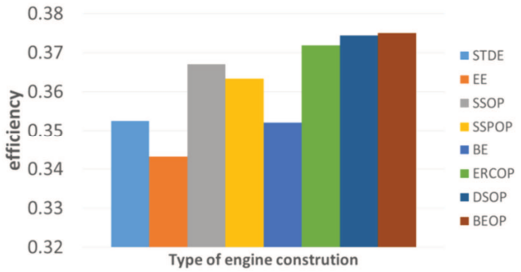

Fig. 17. Comparison of different engine configuration on efficiencies.

For each calculation maximum temperature and maximum pressure was collected. The plots presented at Figures 18 and 19 are showing the peak temperatures and peak pressures for each engine variation for setup 1 (Table 11).

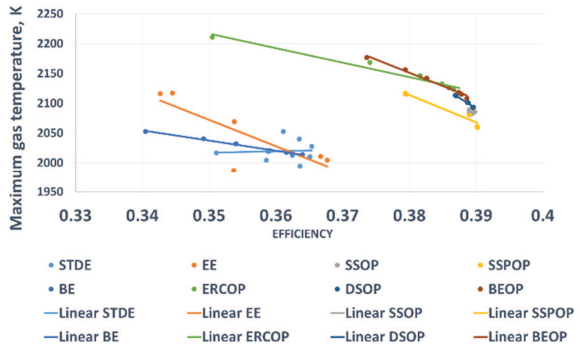

Fig. 18. Maximum gas temperatures for all designs

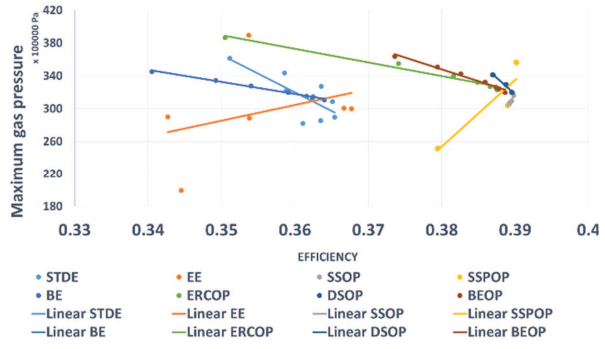

Fig. 19. Maximum gas pressures for all designs

In general the engine configurations shows that for lower peak values of the pressure and temperature the engine shows higher efficiency. Some of the configurations present very good trend for both parameters (BEOP, ERCOP, BE, SSOP, DSOP). The biggest variations are visible for the EE engine and it can be explained by the very different shape of piston curves in comparison to the rest of the engine designs.

The level of peak pressures for the conducted analysis reaches 390 bars while the peak temperatures are for most cases above 2000 K.

Average efficiency of all engine configurations and geometrical variations for setup 4 was 33.8% while for setup 5 was 38.3%.

6. Summary and conclusions

All engine configurations showed that it is beneficial to lower the time of combustion duration. The difference of the average efficiencies between setup 4 and setup 5 reached 5 percentage points. Those setups differs by one parameter which is combustion duration (70 deg CA, 30 deg CA respectively).

Most of the engines configurations presented trend that the lower combustion peak temperature appears in the closed cycle analysis the higher efficiency is. This phenomena can be connected with lower heat losses for the lower gas temperatures. For the whole cycle the wall temperature of the liner, piston and head (not OP engines) was set on the constant level and for those configurations where the peak temperature was higher the more heat was lost to the cooling system.

Regardless of the engine configuration the opposed piston engines proved to have, in general, higher efficiency exceeding for some cases 6% difference.

Optimization of piston motion curves may aid the process if increasing engine efficiency. It was showed that some of the curves indicated lower fuel consumption. The impact of the piston motion curves may be affected by other parameters such us combustion duration or start of combustion. The dependencies between the parameters and efficiency are not linear and the impact of them should be analyzed at the same time.

Acquired gas peak parameters were considered very high. This was connected with high starting pressure (4 bars) and compression ratio on the level of 19. Because of the high temperatures the loss of heat to the walls affected efficiency. In order to increase the efficiency the wall temperatures could be increase and the starting temperature could be lowered.

Due to very unique behavior of EE engine it is recommended to analyze this construction with separate parameters selected for this particular engine.

The construction of the ERCOP engine allows reaching the same number of cycles within particular time for twice lower speed than the other engines. This is a mitigation of the drawback of this construction. Since this design has a high inertia loads due to rotation of the cylinder lower speed may reduce the forces and stresses in this construction.

Nomenclature

CA crank angle
TCD top dead center
BDC bottom dead center
LHV fuel lower heating value
OP opposed-piston

Bibliography

[1] PIRAULT, J-P., FLINT, M. Opposed piston engines: Evolution, use and future applications. *SAE International*. Warrendale, 2010, 7-15.

[2] DZIERŻANOWSKI, P., ŁYŻWIŃSKI, M. Silniki tłokowe. *WKŁ*. Warszawa, 1981, 86-90.

[3] JĘDRZEJOWSKI, J. Mechanika układów korbowych silników samochodowych. *WKiŁ*. Warszawa, 1979, 16-47.

[4] RYCHTER, T. Analiza możliwości podwyższenia sprawności cieplnej silników tłokowych ZI. *Wydawnictwo PW*. Warszawa, 1986, 43-50.

[5] RYCHTER, T., TEODORCZYK, A. VR/LE engine with a variable R/L during a single cycle. *SAE Technical Paper 850206*.1985.

[6] HUO, M., HUANG, Y., HOFBAUER, P. Piston design impact on the scavengine and combustion in an opposed-piston, opposed-cylinder (OPOC) two-stroke engine. *SAE Technical Paper 2015-01-1269*. 2015.

[7] HEROLD, R., WAHL, M. et al. Thermodynamic benefits of opposed-piston two-stroke engines. *SAE Technical Paper 2011-01-2216*. 2011.

[8] KALKE J., OPALIŃSKI, M., SZCZECIŃSKI, M.. Opposed-piston engines: the future of internal combustion engines. *PhD Interdisciplinary Journal,* Gdańsk, 2014. 175-184.

[9] www.cedesign.net/steam/coomber.htm

[10] McBRIDE, B., ZEHE, M., GORDON, S., NASA Glenn coefficients for calculating thermodynamic properties of individual species *NASA/TP – 2002-211556,* 2003.

[11] PUDLIK, W., Termodynamika. *Wydawnictwo Politechniki Gdańskiej*. Gdańsk, 2007, 168.

Marcin Opaliński, MSc. – Faculty of Power and Aeronautical Engineering.

e-mail: *Marcin.Opalinski@itc.pw.edu.pl*

Prof. Andrzej Teodorczyk, DSc., DEng. – Faculty of Power and Aeronautical Engineering.

e-mail: *Andrzej.Teodorczyk@itc.pw.edu.pl*

Jakub Kalke, MSc. – Faculty of Power and Aeronautical Engineering.

e-mail: *Jakub.Kalke@itc.pw.edu.pl*